ACS Photonics

Letter

pubs.acs.org/journal/apchd5

Efficient 10-Fold Upconversion through Steady-State Non-Thermal-Equilibrium Excitation

Dafna Granot,[†] Nimrod Kruger,[†] Assaf Manor,[‡] and Carmel Rotschild*[,†,‡,§]

[†]Grand Technion Energy Program, [‡]Russell Berrie Nanotechnology Institute, and [§]Department of Mechanical Engineering, Technion−Israel Institute of Technology, Haifa 32000, Israel

Supporting Information

ABSTRACT: Frequency upconversion of a few low-energy photons into a single high-energy photon contributes to imaging, light sources, and detection. However, the upconverting of many photons exhibits negligible efficiency. Upconversion through laser heating is an efficient means to generate energetic photons; yet the spectrally broad thermal emission and the challenge of operating at high temperatures limit its practicality. Heating specific modes can potentially generate narrow upconverted emission; however, so far such "hot-carriers" have been observed only in downconversion processes and as having negligible lifetime, due to fast thermalization. Here we experimentally demonstrate upconversion by excitation of a steady-state non-thermal-equilibrium population, which induces steady, narrow emission at a practical bulk temperature. Specifically, we used a 10.6 μm laser to generate 980 nm narrow emission with 4% total efficiency and upconverted radiance that far exceeds the device's possible blackbody radiation. This opens the way for the development of new light sources with record efficiencies.

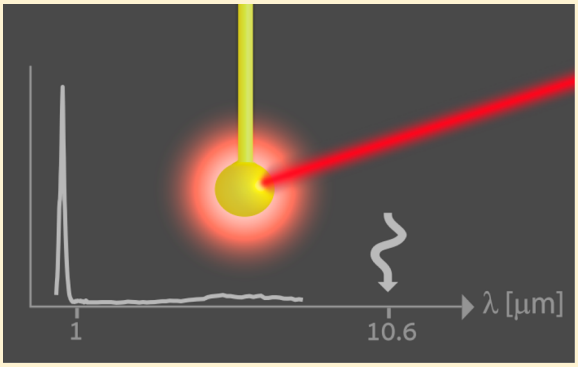

KEYWORDS: *frequency upconversion, nonequilibrium thermodynamics*

Conventional optical frequency upconversion methods include coherent (second, third, and parametric upconversion[1−3]) and incoherent (two-photon[4,5] and multiphoton absorption[6]) processes, which are of major importance in various fields.[1,7,8] Yet, upconversion of many photons (~10) exhibits negligible efficiency, due to the large momentum mismatch between the pump and the produced frequencies in the parametric process,[9] as well as the high intensities required for many photons to interact simultaneously in the multiphoton absorption process. Therefore, the record efficiency of 10-fold upconversion is less than 0.01%, achieved under pulse excitation at intensities of 10^{15} W/cm^2, many orders of magnitude above currently available continuous wave (CW) sources.[10]

A naive approach to efficiently generate high optical frequencies is to use a partially coherent low photon energy pump (such as an infrared laser) to increase a body's temperature, thereby generating thermal radiation with an energetic spectral tail in the visible. Although such heating was shown to be highly efficient,[11,12] it is challenging to implement, as very high temperatures are needed to produce a considerable amount of energetic photons. Moreover, the resulting broad thermal emission is unsuitable for many applications, and its intensity is limited to the blackbody curve. Broad thermal emission can be tailored by various methods,[13,14] but successful demonstration of narrow emission at high temperatures has not yet been achieved. An ideal device would operate efficiently at practical temperatures and emit upconverted light at a narrow spectrum. These ideal guidelines can be met if specific modes are heated to a temperature that is much above the bulk temperature. Such nonthermal radiation is characterized by high radiance above thermal emission at specific frequencies. In the case where these "hot-modes" are highly coupled, they equilibrate the excitation between them and are treated as being in quasi-thermodynamic equilibrium. Their emission is formulated by introducing a scalar chemical potential, μ, into Planck's thermal emission:[15−17]

$$R(\hbar\omega, T, \mu) = \varepsilon(\hbar\omega)\frac{(\hbar\omega)^2}{4\pi^2\hbar^3c^2}\frac{1}{e^{\hbar\omega-\mu/K_BT}-1} \cong R_{\text{thermal}}e^{\mu/K_BT} \quad (1)$$

where R is emitted photon flux (photons per second per unit area per solid angle per frequency), T is temperature, ε is emissivity, $\hbar\omega$ is photon energy, K_b is Boltzmann's constant, and R_{thermal} is Planck's thermal emission. Multiplying R by photon energy results in hemispherical radiance, $L = R\hbar\omega$. Chemical potential, μ, is directly connected to Gibbs free energy: $G = \sum\mu N$ (N being the number of emitted photons with equal μ) and, thus, to the amount of work that can be done with respect to the bulk temperature. A pump at radiance characterized by a high value of μ can spontaneously excite

Received: August 26, 2015
Published: January 28, 2016

DOI: 10.1021/acsphotonics.5b00481
ACS Photonics 2016, 3, 174−178

modes to emit radiance with lower (yet higher than zero) μ levels.

Another description for radiance above thermal emission attributes highly excited modes to a brightness temperature higher than the bulk temperature. Although in such non-equilibrium conditions the term temperature is not well-defined, brightness temperature describes the temperature of a blackbody whose emission at a specific frequency equals that of the emitting mode of interest.[18−20] A body under ideal thermal insulation that absorbs radiation at a given brightness temperature is heated to that temperature. The brightness temperature T_b for a given bulk temperature T, photon energy $\hbar\omega$, and chemical potential μ is $T_b = T\hbar\omega/(\hbar\omega - \mu)$.

Excitation to high brightness temperature was detected over four decades ago in semiconductors,[21] where a short pulsed laser generated "hot-electrons" much above the band gap, with a brightness temperature of 3700 K. This excitation was followed by fast thermalization to the bulk temperature,[22] which remained at 290 K. To the best of our knowledge, the excitation of hot-carriers has been demonstrated only in downconversion configurations, where the pump photon energy exceeded that of the hot-electrons.[10,21] As far as we know, utilization of such ideas for frequency upconversion has never been explored, even though thermalization is driven by free energy (brightness temperature) and not exclusively by photon energy. That is, a mode with a high brightness temperature thermalizes to higher frequency modes at lower brightness temperature, as is regularly done in optical refrigeration.[23] Thermalization continues to other modes until the brightness temperature approaches the bulk temperature at equilibrium.

In a more detailed quantum picture, energy dissipates according to the coupling between modes, which depends, among other parameters, on the density of states as well as on selection rules. An emitter efficiently coupled to the initially excited modes emits spectrally narrow radiation at high brightness temperature, even if the emitted radiation has a higher frequency than the absorbed frequency.

Experimentally, we used a CW CO_2 laser at 10.6 μm wavelength to resonantly pump the vibronic states of silica (Figure 1a). Their high density of states at wavelengths longer than 8 μm induces an absorption cross-section of a few micrometers,[24] leading to high brightness temperatures. Furthermore, silica has a low density of states, and therefore barely radiates, at wavelengths between 0.4 and 5 μm. We doped the silica with rare-earth ions, such as ytterbium (Yb^{3+}, emitting at 980 nm) or neodymium (Nd^{3+}, emitting at 820, 900, and 1064 nm).[11] These rare-earth emitters are often used in optical refrigeration due to their high quantum efficiency of anti-Stokes florescence, where vibronic excitations are coupled with the radiative transition.[23,25] Using these materials in our experiment allows for efficient cascaded energy transfer from the laser pump to the silica and onward to the emitter, even though the emission frequency is higher than that of the pump.

Initially, we demonstrated by experiment the non-thermal-equilibrium nature of such excitation, by comparing the emission of the rare-earth-doped sample under CW CO_2 laser excitation with its thermal emission at high temperature achieved using a furnace (Figure 1b). We connected a 50 μm long Nd^{3+}-doped silica fiber to a passive silica fiber and placed it in a microheater at 1400 °C, the maximal temperature at which the fiber does not deform. The guided emission was measured at the end of the fiber using a calibrated spectrum analyzer (see

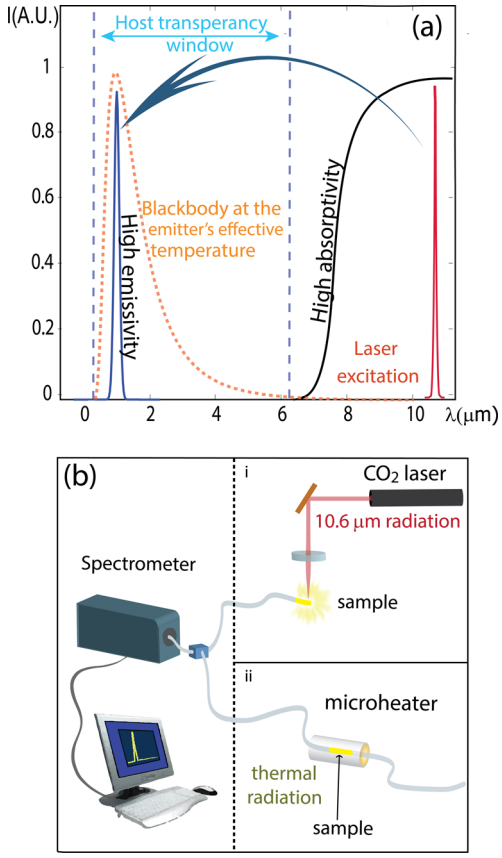

Figure 1. Experimental configuration: (a) CO_2 laser excited the vibrational modes of the silica (10.6 μm), which were coupled with emitting modes of rare-earth ions at about 1 μm. (b) Experimental setup comparing the emission under CO_2 excitation to the sample's thermal emission.

the solid red line in Figure 2a). The extrapolation of this plot to the expected emission at the melting temperature of silica (1650 °C) is depicted by the purple dotted line in Figure 2a (see Methods section for details). This served as an upper limit for thermal radiation of the stable device. The solid blue line in Figure 2a depicts the emission of an equally measured identical sample under CO_2 laser excitation at 0.5 W. The radiance under CO_2 excitation was measured to be 5 times higher than the maximal thermal excitation at the melting temperature. We verified that the sample remained stable throughout dozens of experimental runs.

In addition, we used the fluorescence intensity ratio (FIR) method[26] to determine the brightness temperature of the emitting modes. In this method, the multiple emission peaks of Nd^{3+} (as opposed to Yb^{3+}'s single peak) are exploited to ascertain the temperature, by measuring the radiance ratio between two adjacent peaks (see Methods section for more details). Figure 2b depicts the device's emission spectrum around 1 μm under various CO_2 laser intensities below the melting threshold. The green line shows the brightness temperature at 0.5 W excitation that reaches 2010 °C, 360 deg higher than the bulk melting temperature.

These two different observations indicated that the emitting modes had considerably higher brightness temperature than the bulk temperature.

After confirming the non-thermal-equilibrium nature of our upconversion process we proceeded to examine experimentally

DOI: 10.1021/acsphotonics.5b00481
ACS Photonics 2016, 3, 174−178

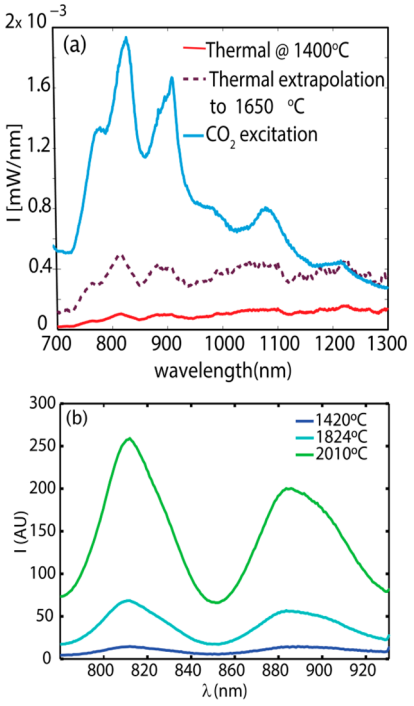

Figure 2. Measurements of nonthermal emission: (a) The emission power spectrum around 1 μm under CW CO_2 excitation (blue line) exceeded that of the measured thermal emission at 1400 °C (red line) and that of the extrapolated thermal emission at the melting temperature of 1650 °C (dotted line). (b) FIR measurements indicated a Nd^{3+} maximal brightness temperature of 2010 °C (green line), much above the maximal possible bulk temperature.

its internal and total efficiencies. Yb_2O_3-doped SiO_2 spherical fiber tips were produced, with diameters between 30 and 300 μm. At a CO_2 power level of 684 mW, the emission image was captured using a Si CCD camera, which is able to detect wavelengths shorter than 1.1 μm, in order to gain information on the size of the emitting area, essential for calculating the radiance. A typical image, with an emitting area of 10^{-8} m^2, is shown in the inset of Figure 3. Next, the sample's spectral radiance between 0.4 and 11 μm wavelength was detected by

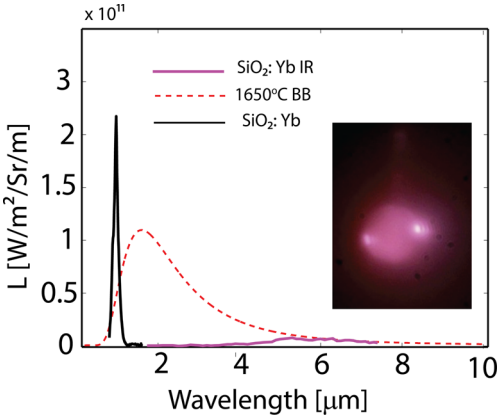

Figure 3. Spectral measurements of the Yb_2O_3-doped silica under CO_2 excitation. Measured power spectrum (black and pink line) indicates 27% internal efficiency and surpasses a theoretical blackbody radiance at 1650 °C (dotted red line), the melting temperature of the bulk. This implies a high brightness temperature of the Yb_2O_3's emitting modes compared to the bulk temperature.

exciting the sample within an integrating sphere connected to a spectrograph and calibrated against a calibration lamp and a blackbody source at 1200 °C (see Methods section). Normalizing the spectral radiance with the emission area resulted in a minimal value for radiance, assuming isotropic emission (see solid lines in Figure 3).

Our measurements resulted in a sharp, narrow peak at 980 nm attributed to the ytterbium emission, which included 27% of all the total emittance, indicating relatively high internal efficiency. Residual broad emission, from approximately 5 to 8 μm, originated from silica's highly emissive spectral region and fits the theoretical blackbody curve at 1650 °C, just below the bulk melting temperature (red dotted line in Figure 3). The Yb_2O_3 emission at 980 nm peak was measured as four times higher than this theoretical curve, implying that while the bulk was stable just below 1650 °C, the brightness temperature of theYb_2O_3 was about 2050 °C.

Finally, external efficiency was determined by placing the setup in a vacuum chamber at 10^{-3} Torr, in order to reduce thermal losses. The Yb_2O_3 emission power at the 980 nm peak was measured at various CW CO_2 power levels. Efficiency was calculated as the ratio between the measured absorbed CO_2 power and the measured Yb_2O_3 emission power (Figure 4 dots). The resulting maximal external efficiency approached 4%, where 1.75 mW of Yb_2O_3 radiation was detected under 49 mW CO_2 pump intensity.

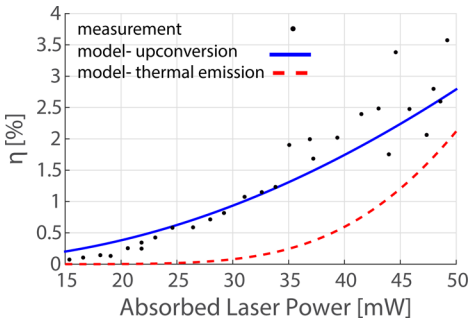

Figure 4. Total efficiency of the Yb_2O_3-doped silica at various CO_2 power levels under vacuum (black dots). The maximal efficiency achieved was over 3.5%, many orders of magnitude better than prior reports. The trend fits a simulation (blue line) based on a quantum-thermodynamic model of rare-earth emission. Calculated thermal radiation (red dashed line) shows inferior results.

The efficiency trend is in accord with a model based on Torsello's quantum-thermodynamic theory of thermal pumping and radiative de-excitation in rare-earth oxide materials[27] (Figure 4 blue line), using our experimental parameters (see Supporting Information). For these parameters, the model also predicts a maximal possible efficiency of about 4%, slightly above our measured value, where the emission becomes thermal. Moreover, the dashed line in Figure 4 predicts lower efficiency for an equivalent sample in an equilibrium state, confirming the supremacy of the upconversion over thermal emission.

A further experiment presented in the Supporting Information shows the sample's emission lifetime to be 12–14 ms, longer than the typical Yb^{3+} photoluminescence lifetime of about 1 ms.[28] This can be explained by the delaying effect of the cascaded energy transfer.

To conclude, we presented a new frequency upconversion mechanism driven by excitation of hot radiative modes, where

DOI: 10.1021/acsphotonics.5b00481
ACS Photonics 2016, 3, 174–178

the emission under resonant excitation exceeded the maximal possible thermal emission. Specifically, we experimentally demonstrated a 10-fold upconversion from CO_2 emission at 10.6 to 1 μm at an internal efficiency of 27% and total efficiency of almost 4%, orders of magnitude higher than current state-of-the-art. The efficiency can be further improved using different materials and excitation wavelengths, along with conventional methods for tailoring thermal emission such as photonic band-gap structures. This method may open new directions in various fields of research, such as new light sources and solar energy, where efficiency can be enhanced by upconverting sub-band-gap solar photons to wavelengths where photovoltaics are most efficient.

METHODS

Experiment: Upconversion Compared with Thermal Emission. *Sample Preparation.* A 125 μm Nd-doped silica optical fiber (CorAcrive) was stripped and connected using an Ericsson fusion splicer to a matched passive silica fiber. The active fiber was then cut to a length of 50 μm and connected to another passive fiber, resulting in a 50 μm active fiber inserted between two long (~50 cm) passive fibers.

Thermal Emission Measurement. The fiber was inserted into a high-temperature microheater (Micropyretics Heater Instruments, Inc.), with the Nd-doped section in the middle of the oven, held by translation stages at the two outer sides. One side of the fiber was coupled to a monochromator (Andor) with an InGaAs camera (Andor), calibrated using a calibration lamp (Oriel Instruments). During the experiment, the temperature was gradually elevated to 1400 °C, and the emission at 0.7−1.5 μm was recorded. The background emission was then measured by pulling the active fiber out of the heater, having only the passive part heated; thus the measured signal originated solely from the heater. Extrapolation of the result to 1650 °C was conducted by multiplying it by $\frac{R(\hbar\omega, 1400\,^\circ\mathrm{C})}{R(\hbar\omega, 1650\,^\circ\mathrm{C})}$, calculated from eq 1, with $\mu = 0$.

Upconversion Emission Measurement. An identical sample was connected to a passive fiber coupled to the monochromator. The 50 μm Nd-doped fiber tip was pumped by a CW CO_2 laser (Access Lasers) at less than 1 W, and measurements were taken at the same conditions as in the previous case. When the CO_2 laser was focused on the passive fiber, no emission was detected.

FIR Experiment. Within a narrow spectral band where the chemical potential is assumed to be equal, the ratio between two adjacent luminescent peaks is defined by Boltzmann distribution:

$$R = C(\Delta E)\, e^{-\Delta E/K_b T} \tag{2}$$

where ΔE is the energy difference between the two levels—900 and 820 nm—and $C(\Delta E)$ is a constant that can be found by calibration.[26]

Calibration. In order to ascertain $C(\Delta E)$, an active Nd-doped fiber was inserted into a long matching passive fiber as described in section 1, and the active part was put into the microheater. One side of the fiber was coupled to the monochromator with the InGaAs camera, while the other side was pumped by a 532 nm laser. The temperature was increased gradually, with a measurement taken for each temperature, whereby intensities of 820 and 900 nm were recorded and the ratio between them was calculated. A calibration plot was made using data from these measurements (I_{900}/I_{820} vs $T(C)$), and C was extracted and found to be 0.4. Without the 532 nm pump, the thermal signal was too weak for detection. Equation 1 and ref 14 show how photoluminescence has a relative spectrum identical to that of thermal emission.

Measurements. A Nd-doped fiber of the type used for the calibration was pumped by the CO_2 laser, and its emitted radiation was detected in free space using a Si detector (Ocean Optics). Measurements were taken for different laser powers under 1 W. The ratio I_{900}/I_{820} was derived from the measurements and inserted into eq 2 to obtain the temperature.

Efficiency Experiments. *Sample Preparation.* Two types of samples were used. The first one was Yb-doped commercial 500 μm fibers (CorActive). The second type was a sphere at a fiber tip, made by the following method: 125 μm fibers (Thorlabs) were positioned in the focus of a CO_2 laser (Synrad). The fiber tip was melted and fed into the focal point until the formation of a sphere. Subsequently, the sphere was dip-coated in methanol Yb_2O_3 nanocrystals in suspension (1 mL methanol/100 mg Yb_2O_3) and then melted again by a short laser exposure of about half a second, in order to gain a smooth surface sphere and uniform Yb_2O_3 concentration. For smaller spheres, the fibers were etched in an HF/H_2O solution prior to the melting process, until the desired diameter was reached.

Measurements. Sample radiance was measured using an integrating sphere (LabSphere for the NIR range and a custom-made gold-coated sphere for the infrared range). A CW CO_2 laser with 2% stability (Access Lasers) at various intensities (measured using a power meter) was focused onto the sample by a gold parabolic mirror and ZnSe lens. In addition, a calibration lamp (Newport) and a 1200 °C calibrated blackbody source (CI Systems) were directed into the sphere for calibration purposes. The luminescence signals were chopped by an optical chopper (Stanford Research Systems) and amplified by a lock-in amplifier (Stanford Research Systems) after passing through a spectrograph equipped with the appropriate gratings for the different spectral ranges (Oriel Instruments). In the near-infrared region, signals were measured by a Ge detector (Judson Technologies) and an InGaAs camera (Andor Technology). In the infrared region between 2 and 10 μm, signals were detected using InSb and MCT (InfraRed Associates) detectors.

ASSOCIATED CONTENT

Supporting Information

The Supporting Information is available free of charge on the ACS Publications website at DOI: 10.1021/acsphotonics.5b00481.

Lifetime measurements; semiempirical model for the upconversion external efficiency (PDF)

AUTHOR INFORMATION

Corresponding Author

*E-mail (C. Rotschild): carmelr@tx.technion.ac.il. Tel: +927-77-887-1740.

Author Contributions

The first three authors contributed equally to this paper.

Notes

The authors declare no competing financial interest.

ACKNOWLEDGMENTS

This report was partially supported by the Russell Berrie Nanotechnology Institute (RBNI) and the Grand Technion

DOI: 10.1021/acsphotonics.5b00481
ACS Photonics 2016, 3, 174−178

Energy Program (GTEP) and is part of The Leona M. and Harry B. Helmsley Charitable Trust reports on Alternative Energy series of the Technion and the Weizmann Institute of Science. We also would like to acknowledge partial support by the Focal Technology Area on Nanophotonics for Detection. A.M. thanks the Adams Fellowship program for financial support. C.R. thanks the Marie Curie European reintegration grant for its support.

REFERENCES

(1) Lucy, R. F. Infrared to Visible Parametric Upconversion. *Appl. Opt.* **1972**, *11*, 1329−1336.
(2) Warner, J. Parametric up-Conversion from the Infra-Red. *Opt. Quantum Electron.* **1971**, *3*, 37−48.
(3) Yariv, A. *Quantum Electronics*, 3rd ed.; Wiley, 1989.
(4) Shalav, A.; Richards, B. S.; Trupke, T.; Krämer, K. W.; Güdel, H. U. Application of NaYF4:Er3+ up-Converting Phosphors for Enhanced near-Infrared Silicon Solar Cell Response. *Appl. Phys. Lett.* **2004**, *86*, 013505−013505-3.
(5) Baluschev, S.; Miteva, T.; Yakutkin, V.; Nelles, G.; Yasuda, A.; Wegner, G. Up-Conversion Fluorescence: Noncoherent Excitation by Sunlight. *Phys. Rev. Lett.* **2006**, *97*, 143903.
(6) Auzel, F. Upconversion and Anti-Stokes Processes with F and D Ions in Solids. *Chem. Rev.* **2004**, *104*, 139−174.
(7) Denk, W.; Strickler, J. H.; Webb, W. W. Two-Photon Laser Scanning Fluorescence Microscopy. *Science* **1990**, *248*, 73−76.
(8) Vandevender, A. P.; Kwiat, P. G. High Efficiency Single Photon Detection via Frequency up-Conversion. *J. Mod. Opt.* **2004**, *51*, 1433−1445.
(9) Trupke, T.; Green, M. A.; Wurfel, P. Improving Solar Cell Efficiencies by up-Conversion of Sub-Band-Gap Light. *J. Appl. Phys.* **2002**, *92*, 4117−4122.
(10) Carman, R. L.; Rhodes, C. K.; Benjamin, R. F. Observation of Harmonics in the Visible and Ultraviolet Created in CO_2-Laser-Produced Plasmas. *Phys. Rev. A: At., Mol., Opt. Phys.* **1981**, *24*, 2649−2663.
(11) Guazzoni, G. E. High-Temperature Spectral Emittance of Oxides of Erbium, Samarium, Neodymium and Ytterbium. *Appl. Spectrosc.* **1972**, *26*, 60−65.
(12) Wang, J.; Ming, T.; Jin, Z.; Wang, J.; Sun, L.-D.; Yan, C.-H. Photon Energy Upconversion through Thermal Radiation with the Power Efficiency Reaching 16%. *Nat. Commun.* **2014**, *5*.566910.1038/ncomms6669
(13) De Zoysa, M.; Asano, T.; Mochizuki, K.; Oskooi, A.; Inoue, T.; Noda, S. Conversion of Broadband to Narrowband Thermal Emission through Energy Recycling. *Nat. Photonics* **2012**, *6*, 535−539.
(14) Celanovic, I. Design and Global Optimization of High-Efficiency Solar Thermal Systems with Tungsten Cermets. *Opt. Express* **2011**, *19*.A24510.1364/OE.19.00A245
(15) Ross, R. T. Some Thermodynamics of Photochemical Systems. *J. Chem. Phys.* **1967**, *46*, 4590−4593.
(16) Wurfel, P. The Chemical Potential of Radiation. *J. Phys. C: Solid State Phys.* **1982**, *15*, 3967−3985.
(17) Ries, H.; McEvoy, A. J. Chemical Potential and Temperature of Light. *J. Photochem. Photobiol., A* **1991**, *59*, 11−18.
(18) Weinstein, M. A. Thermodynamic Limitation on the Conversion of Heat into Light. *J. Opt. Soc. Am.* **1960**, *50*, 597.
(19) Landsberg, P. T.; Evans, D. A. Thermodynamic Limits for Some Light-Producing Devices. *Phys. Rev.* **1968**, *166*, 242−246.
(20) Landsberg, P. T.; Tonge, G. Thermodynamic Energy Conversion Efficiencies. *J. Appl. Phys.* **1980**, *51*, R1−R20.
(21) Gallego Lluesma, E.; Mendes, G.; Arguello, C. A.; Leite, R. C. C. Very High Non-Thermal Equilibrium Population of Optical Phonons in GaAs. *Solid State Commun.* **1974**, *14*, 1195−1197.
(22) Lyon, S. A. Spectroscopy of Hot Carriers in Semiconductors. *J. Lumin.* **1986**, *35*, 121−154.
(23) Sheik-Bahae, M.; Epstein, R. I. Optical Refrigeration. *Nat. Photonics* **2007**, *1*, 693−699.
(24) Rozenbaum, O.; Meneses, D. D. S. A Spectroscopic Method to Measure the Spectral Emissivity of Semi-Transparent Materials up to High Temperature. *Rev. Sci. Instrum.* **1999**, *70*, 4020−4025.
(25) Seletskiy, D. V.; Melgaard, S. D.; Bigotta, S.; Di Lieto, A.; Tonelli, M.; Sheik-Bahae, M. Laser Cooling of Solids to Cryogenic Temperatures. *Nat. Photonics* **2010**, *4*, 161−164.
(26) Wade, S. A.; Collins, S. F.; Baxter, G. W. Fluorescence Intensity Ratio Technique for Optical Fiber Point Temperature Sensing. *J. Appl. Phys.* **2003**, *94*, 4743−4756.
(27) Torsello, G.; Lomascolo, M.; Licciulli, A.; Diso, D.; Tundo, S.; Mazzer, M. The Origin of Highly Efficient Selective Emission in Rare-Earth Oxides for Thermophotovoltaic Applications. *Nat. Mater.* **2004**, *3*, 632−637.
(28) Paschotta, R.; Nilsson, J.; Barber, P. R.; Caplen, J. E.; Tropper, A. C.; Hanna, D. C. Lifetime Quenching in Yb-Doped Fibres. *Opt. Commun.* **1997**, *136*, 375−378.

DOI: 10.1021/acsphotonics.5b00481
ACS Photonics 2016, 3, 174−178